ACS SyntheticBiology

pubs.acs.org/synthbio Review

Motility of Synthetic Cells from Engineered Lipids

Published as part of the ACS Synthetic Biology virtual special issue "Synthetic Cells".

Aishwary Shrivastava, Yancheng Du, Harshith K. Adepu, Ruixin Li, Anirudh S. Madhvacharyula, Alexander A. Swett, and Jong Hyun Choi*

Cite This: *ACS Synth. Biol.* 2023, 12, 2789−2801 Read Online

ACCESS | Metrics & More | Article Recommendations

ABSTRACT: Synthetic cells are artificial systems that resemble natural cells. Significant efforts have been made over the years to construct synthetic protocells that can mimic biological mechanisms and perform various complex processes. These include compartmentalization, metabolism, energy supply, communication, and gene reproduction. Cell motility is also of great importance, as nature uses elegant mechanisms for intracellular trafficking, immune response, and embryogenesis. In this review, we discuss the motility of synthetic cells made from lipid vesicles and relevant molecular mechanisms. Synthetic cell motion may be classified into surface-based or solution-based depending on whether it involves interactions with surfaces or movement in fluids. Collective migration behaviors have also been demonstrated. The swarm motion requires additional mechanisms for intercellular signaling and directional motility that enable communication and coordination among the synthetic vesicles. In addition, intracellular trafficking for molecular transport has been reconstituted in minimal cells with the help of DNA nanotechnology. These efforts demonstrate synthetic cells that can move, detect, respond, and interact. We envision that new developments in protocell motility will enhance our understanding of biological processes and be instrumental in bioengineering and therapeutic applications.

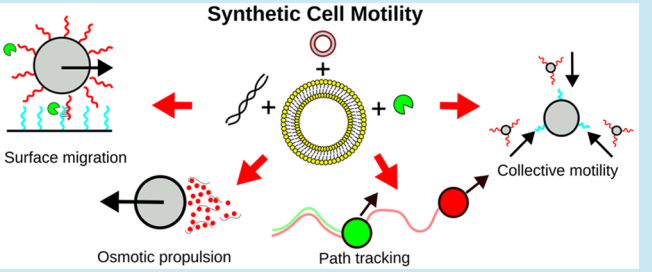

KEYWORDS: *synthetic cells, vesicles, lipids, motility, DNA self-assembly, DNA nanotechnology*

1. INTRODUCTION

Cells are the basic building blocks of life. Naturally occurring cells are complex membrane-bound entities containing various fundamental molecules that are required to keep an organism alive.[1,2] In order to study the origins of life and evolutionary processes, artificial replications of the first primitive cells were developed, called synthetic or artificial cells.[2,3] Thus, protocells can be defined as chemical systems designed to mimic the structure, behavior, and functions of natural cells.[4] Ganti's chemoton model states that for an artificial cell to describe life, it must contain a chemical boundary system (such as lipid membrane), metabolic units, and self-replicating machinery.[1,5,6] It may also include mechanisms for environmental adaptivity as well as growth and division. Building synthetic cells from scratch, that can perform certain specific functions is called the bottom-up approach.[4] This bottom-up approach offers full control over their functions and structure, unlike top-down methods where some components are removed from natural cells to construct protocells.[3,4] From an engineering point of view, bottom-up design is easier for embedding molecular machineries in protocells and applying physical principles in artificial systems. Several forms of synthetic cells have been developed using this approach,[2,7] including lipid vesicles,[8−10] colloidosomes,[11] proteinosomes,[12,13] capsosomes,[14] dendrimersomes,[15] polymersomes,[16−18] and coacervate droplets.[19] Because of the structural similarities of liposomes to cell membranes and their ability to incorporate functional macromolecules into their membranes, vesicles have been extensively used.[4,20] They can also be produced in a variety of sizes (0.02 to 100 μm) based on the synthesis methods.[21] Hence, in this review, we focus our discussion on synthetic cells produced by vesicles using the bottom-up approach.

To date, several major cellular functions have been reconstituted in artificial cells. Compartmentalization is needed for storage, protection, and processing of vital molecules.[22,23] For example, liposome-in-liposome compartment systems have been developed by incorporating small unilamellar vesicles (SUVs) inside giant unilamellar vesicles (GUVs).[24] Gene expressions were also demonstrated within synthetic cells using riboswitches and encapsulated transcription systems were used

Received: April 30, 2023
Published: September 20, 2023

https://doi.org/10.1021/acssynbio.3c00271
ACS Synth. Biol. 2023, 12, 2789−2801

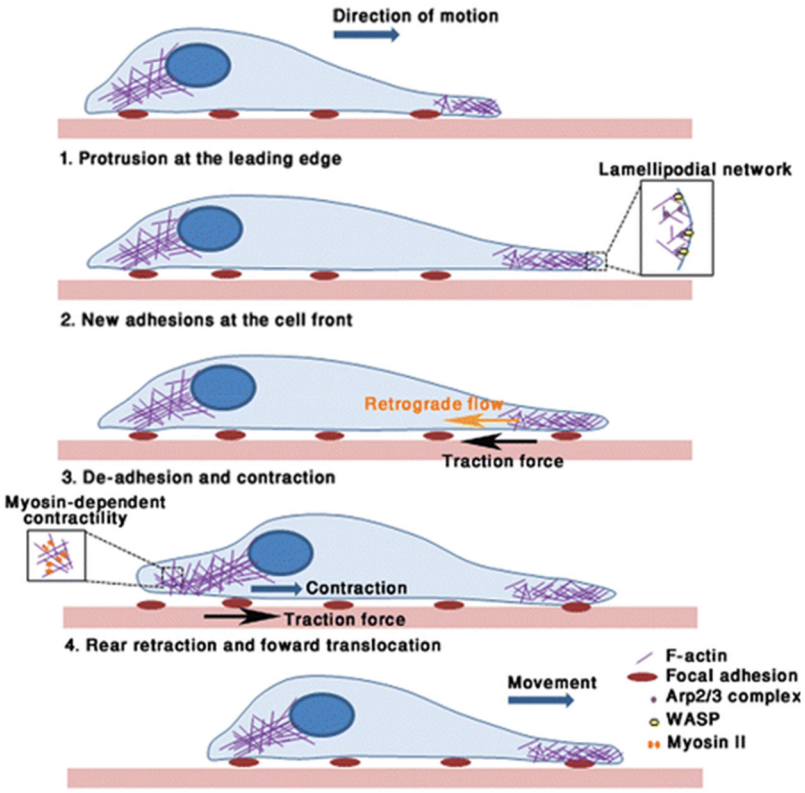

Figure 1. Illustration of the steps involved in the motion of a cell on a 2D surface. The motion consists of (1) formation of membrane protrusions at the leading edge, (2) adhesion of the formed protrusions at the front, (3) myosin-dependent contraction along with detachment of rear adhesion points, and (4) rear edge retraction and forward movement of the cell. Reprinted with permission from ref 43. Copyright 2016 Taylor & Francis.

to reconstitute protein synthesis.[25−27] In addition, natural cells communicate via chemical signaling which inspired the development of synthetic cells that could send and detect chemical signals to a group of bacteria.[28] Mechanisms for growth and division of vesicles include producing or depleting membrane molecules.[29−31] Lastly, cell motility is a critical function for numerous biological processes including immune response, material transport, embryonic development, and wound healing.[32−35] Several mechanisms have been introduced to determine the motility of protocells. For example, enzymatic reactions[36] and controlled adhesion between substrates[37] were proposed to create the vesicular motility. While multiple articles have surveyed the recent progress in the protocell functions and motility,[2−4,38] the motility of lipid vesicles has been much less discussed.

Herein, we overview molecular mechanisms that enable the motility of artificial cells. First, we gain insight and take inspiration from natural motility mechanisms. Biological cell motility is usually governed by the action of actin, tubulin, and associated intracellular motors. Next, we elucidate the mechanisms of synthetic cell motility. Motility is classified into surface migration based on the vesicle interactions with substrates and solution-based motion in fluids. Surface migration includes crawling, morphology change, and incorporation of DNA or protein-based machinery, whereas solution-based motility involves motion by propulsion forces generated from chemical reactions or artificial flagella. Cell motility can also be classified into single cell motion and collective behavior. In single cell migration, motility is uncoordinated, whereas in collective motion, local interactions occur to coordinate the movement of protocells. We also discuss designs and functions for mimicking intracellular trafficking, which is essential to transport materials within the cell. Finally, we highlight the methods of characterization and analysis for studying synthetic cell motility. Lastly, we survey exciting applications based on the motility of artificial cells. Overall, this review will shed insight into novel molecular mechanisms for vesicular motility which can open new opportunities.

2. MOTILITY MECHANISMS

2.1. Biological Cells. For a living organism to function, both the external macroscopic motion of bodies and microscopic transport of organelles inside cells are essential. Some cells rely on external driving forces to move (such as red blood cells), while others use internal mechanisms (such as bacteria). Most complex and vital cellular functions are also facilitated by the movement of internal and external organelles. Thus, it is important to understand the mechanisms of cell motility. Motility may be considered as a 4-step process working in tandem: signal generation, detection, transmission, and execution.[32] They can have different mechanisms like flagellar motion (in bacteria and sperm cells[39]) and penetrating into ducts to move from bloodstream to tissue (in neutrophils[40]). The flagellar motion in bacteria is powered by motor proteins located in the basal body of the flagella, which convert energy from an ion gradient across the cell membrane into mechanical energy to rotate the flagella.[41] The direction of rotation is controlled by switch proteins that work in association with motor proteins to produce motion. This mechanism allows bacteria to respond to external signals and navigate their environment.

https://doi.org/10.1021/acssynbio.3c00271
ACS Synth. Biol. 2023, 12, 2789−2801

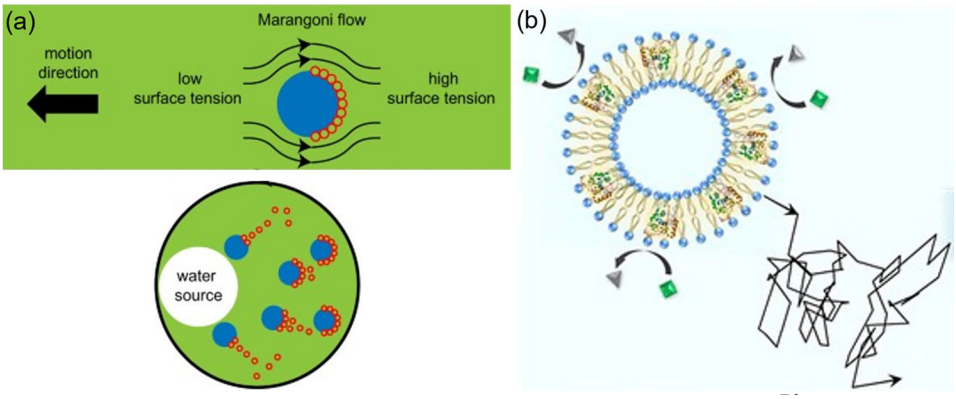

Figure 2. (a) The motility design of the vesicle-surrounded droplets. The solution is depicted in green color, which shows a PEG-rich phase. The blue droplet is a dextran-rich phase. The vesicles (shown in red color) can aggregate at the interfaces. If the biased aggregation forms, the droplet will be pushed by the Marangoni flow and has directional motion. This is introduced by a water source in the system that causes the vesicles to move away and pushes the droplet toward it. Reprinted with permission from ref 70. Published by 2021 Springer Nature Ltd. (b) Schematic of an enzyme-powered synthetic cell. The lipids include biotin and can be combined with biotinylated enzyme (e.g., ATPase) via biotin−streptavidin chemistry. ATPase consumes ATP molecules and generates motility for the protocell, illustrated as the trajectory. Reprinted with permission from ref 72. Copyright 2019 American Chemical Society.

Another important mechanism is the cytoskeletal system where actin proteins form filaments and polymerize at the leading end, thereby moving the cell.[42] This motility has multiple codependent steps as illustrated in Figure 1: (1) membrane protrusions are formed at the leading edge, (2) adhesion of protrusions to the surface, and (3) body contraction along with the detachment of the rear-edge adhesion points.[43] These steps are responsible for forward cell propulsion. The membrane and the cytoskeleton are linked by either membrane proteins or physical interactions between lipids and filaments. This linkage helps the cytoskeleton apply protrusive forces to push membrane outward and contractile forces to pull membrane inward.[44] Polymerization of actin filaments at the leading edge is the driving force for the extension of the membrane protrusions.[45] Adhesive forces are needed to balance the propulsive forces (by actin polymerization) and contractile forces (by mysoin motors).[46]

Motor proteins play a critical role in intracellular motility. Myosin binds to actin filaments and converts chemical energy to mechanical work through a series of conformational changes. When bound to actin, myosin motors hydrolyze ATP and give it a push. The addition of ATP docks off the myosin from actin and redocks with the next actin available. Thus, myosin motors undergo a constant cycle of attachment and detachment from the actin filament.[47] Dynein and kinesin motors travel along microtubules, which are long chains made of tubulin and work as tracks for transporting cargo inside the cell. Tubulin binds to other microtubules in a manner that induces polarity to the track and creates "plus" and "minus" ends.[48] Kinesin delivers cargo from the centrosome (plus end) whereas dynein motors move it toward the cell interior (minus end).[49] These motors are also driven by ATP hydrolysis. Unlike myosin, however, two motor domains of kinesin walk in a coordinated manner (e.g., 8 nm step with a hand-overhand mechanism[50]) and take one step for a cycle of ATP reaction.[51] Dynein has motor domains several times larger than those of kinesin and does not exhibit regular movements.[52,53] Dynein exhibits a wormlike motion pattern where two motor domains maintain front and rear positions and both domains step forward. Thus, its motility is very irregular with different step sizes, timing steps, and backward steps.[54]

2.2. Synthetic Cells. Inspired by various mechanisms of biological cell motility,[2,55] synthetic cells with motility have been introduced in protocell research.[38,56−59] The design of protocell motion can be categorized into solution-based motion and surface-based movement. Solution-based motions are common for biological cells in fluids (e.g., blood or water); this type of motility overcomes resistance from surrounding fluids. This motility commonly involves flagella rotation or an enzymatic reaction to generate propulsion. Such mechanisms have also been mimicked in synthetic cells. Surface-based movement, on the other hand, is related to interactions with surfaces. Natural cells often crawl, which involves constant attachment and detachment from the substrates and usually combines with morphology changes of membranes. Such insight leads the way toward various mechanisms developed for surface-based motility of synthetic cells.

Motility in Free Solution. To create motility in free solution, synthetic cells need to generate forces to push through the liquid. A variety of potential mechanisms may be applied including electrostatic force,[60] magnetic propellant,[61] chemical gradient,[62] enzymatic reaction,[63−66] and surface tension based Marangoni effect.[67−69] In recent studies, successful demonstrations of vesicle motility have been concentrated in mechanisms involving enzymatic reactions or Marangoni effects. For example, Ces et al. proposed a unique mechanism where polyethylene glycol (PEG) and dextran were separated into PEG-rich and dextran-rich phases, where dextran-rich droplets are formed.[70] With the introduction of lipids, liposomes form at the interfaces between PEG-rich and dextran-rich phases and surround the dextran-rich droplets. Then, a water source was introduced in the solution, which caused the liposomes to redistribute around the droplets forming an asymmetric pattern. As depicted in Figure 2a, the asymmetric distribution of vesicles results in a difference in surface tension around the droplets where the side with more liposomes has high surface tension and the other side has low surface tension. The surface tension difference, called the Marangoni effect, generates a flow around the droplet pushing them toward the water source. The effects of the unbalanced vesicles and the type of liposomes were studied, and enhanced motility was demonstrated with an increased vesicle concen-

https://doi.org/10.1021/acssynbio.3c00271
ACS Synth. Biol. 2023, 12, 2789−2801

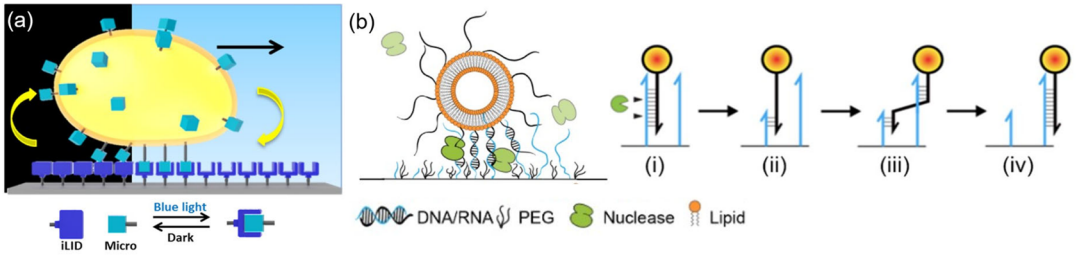

Figure 3. (a) Schematic of light guided movement. iLID and Micro proteins connect the giant vesicle to the substrate. They conjugate under photoirradiation and detach in dark. The light guidance results in the vesicles moving toward the light source. Reprinted with permission from ref 75. Copyright 2018 American Chemical Society. (b) Enzyme-powered surface migration of a protocell with DNA components. Blue sequences are RNA fuels. DNA walkers functionalized on the vesicle are shown in black. (i) Initial DNA/RNA hybridization. (ii) RNase enzyme (green) cleavage of the bound RNA fuel. (iii) The DNA moves to the next available fuels for migration (iv). Reprinted with permission from ref 98. Copyright 2021 American Chemical Society.

tration. The Marangoni effect can provide consistent movement for the synthetic cells, and due to its asymmetric nature, it is possible to design directional or chemotactic behavior of the protocells. However, the drawbacks include limited synthesis methods as well as the requirement of specific solution environments. In another set of studies, Testa et al.[71] proposed the use of pH-driven Marangoni flows to study enzymes in environments that simulate the activity of the cytoplasm.

Sen and co-workers used ATPase to build enzyme-powered vesicles (Figure 2b).[72] In their experiments, small vesicles (~100 nm) included biotinylated lipids that can bind with streptavidin. The ATPase enzymes were also modified with biotin; thus, the vesicles and ATPase can conjugate via the biotin−streptavidin interaction. Fluorescent markers were also included for optical imaging. The ATPase converts ATP to ADP and pumps Na^+/K^+. This process creates a propulsion effect and enhances the motility of vesicles decorated with ATPases. The results showed stark differences in diffusion coefficients in the presence and absence of ATP substrates. They also demonstrated that other enzymes like urease[73] can produce similar motilities as ATPase. The Sen group further expanded the scheme to demonstrate chemotactic behavior of synthetic cells in solution.[74] The vesicles coated with enzymes were introduced into microfluidics with a gradient of corresponding substrates. The concentration difference across the vesicle causes an imbalance in the propulsion force generated by enzymatic reactions, resulting in chemotactic behaviors. They also showed that this simple strategy of biotin−streptavidin binding is versatile for the incorporation of different enzymes on the liposome, which enables positive and negative chemotaxis induced using different enzymes. For example, catalase-coated vesicles move toward a high substrate concentration, whereas urease-coated liposomes move away from the substrate. This enzyme-driven movement demonstrates a strong potential for more sophisticated chemotactic behaviors in artificial cells.

Despite the exciting progress, the development of vesicular motility is still limited. The main obstacles in building lipid-based synthetic cells with motility lie in two areas. First, it is now possible to design vesicles with various sizes and functional groups, yet the methods for coupling lipids with electrostatic, magnetic, or enzymatic units are limited and lack stability. Second, asymmetric designs may be required to create propulsion. Current synthesis methods can contain various compartmentalized segments; however, well controlled localizations in an asymmetric manner are still underdeveloped. We envision that the progress in novel designs and synthesis methods will greatly benefit the solution-phase motility of synthetic cells.

Surface Migration. Apart from motions in solution, natural cells also demonstrate fascinating movement across substrates using morphology change. The morphological changes enable directional motility, while repetitive attachment and detachment from the surfaces can facilitate autonomous motion. For synthetic cells, morphology changes have been realized with composition changes as well as actin cross-linking. For example, Wegner et al. reported a design for light-guided motility of synthetic cells (Figure 3a).[75] They incorporated a pair of proteins named iLID and Micro that interact with each other under blue light (488 nm) and dissociate in the dark. The Micro proteins were coupled to GUVs via His-tag-Ni^{2+}-NTA interaction. The vesicles contain lipids with Ni^{2+}-NTA modified headgroup, and the protein is with His-tag. Similarly, the iLID proteins were coupled on the surfaces where the glass substrates were coated with the Ni^{2+}-NTA group. Thus, the protocells can adhere at locations irradiated by the blue light and detach in the absence of illumination. With the guidance of light, the vesicles demonstrated processive motion across the surface. A movement speed of ~80 nm/s was reported, though a limited number of samples were investigated. This light-guided scheme is highly advantageous with remote directionality control which could be useful for realizing directed delivery and other applications.

Recently, all-synthetic DNA motors have emerged with development of DNA nanotechnology,[76,77] which may be exploited to create directed motility for artificial cells. DNA self-assembly demonstrated the ability to construct complex nanostructures with excellent programmability and structural predictability as well as dynamic control.[78−83] DNA walkers are nanostructured motifs designed to make processive movements by converting chemical energy into mechanical work, similar to protein motors.[84] They use fuel strands made of DNA, RNA, or their combinations. Their translocation dynamics have been explored for programmed migration,[85−87] which can range from tens of nanometers to several micrometers with a speed on the scale of few nm/s.[88−90] Various mechanisms have been developed for these motors including nonautonomous methods such as sequential strand displacement[85,86,91] or autonomous designs such as enzymatic cleavage.[92−96] For example, Salaita and co-workers introduced a cog-wheel type mechanism that propels DNA-modified micrometer-sized spheres.[88] Here, RNA fuel strands were decorated densely on a gold film, and the digestion of the fuel

https://doi.org/10.1021/acssynbio.3c00271
ACS Synth. Biol. 2023, 12, 2789−2801

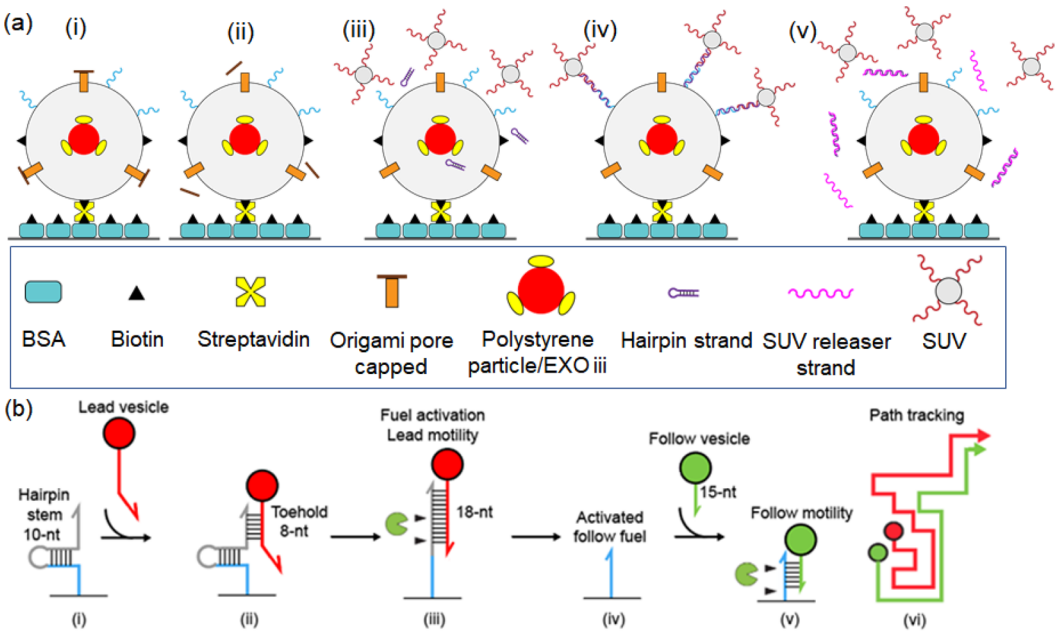

Figure 4. (a) DNA programmed aggregation of SUVs on GUVs. (i) A GUV immobilized on the surface. (ii) Opening of the pores, initially closed with origami caps, by the action of "cap-releaser" strands. (iii) An external DNA hairpin signal enters the GUV and transforms into another signal by Exo III enzyme. (iv) The processed signaling molecules pass through the origami pores and trigger the aggregation of SUVs on the GUV. (v) "SUV releaser" strands dissociate the SUVs from the GUV by removing the linker strands. Reprinted with permission from ref 109. Copyright 2021 American Chemical Society. (b) Coordinated migration of vesicles with a path tracking design. The lead vesicle (shown in red) initially binds with the hairpin fuel (gray). The binding opens the fuel which is then cleaved by the enzyme, moving the lead vesicle. The opened (activated) fuel can then be used by the follow vesicle (green) which then tracks the trajectory of the lead. Reprinted with permission from ref 112. Copyright 2019 American Chemical Society.

strands rolled the particles. This self-avoiding scheme demonstrated speeds significantly higher than those of typical DNA walkers based on strand displacement. The excellent performance was attributed to the multivalency of DNA molecules on the particles. In general, DNA motors are highly programmable such that they can respond to various environmental cues including pH, ionic strength, and light signal.[97] Further, they may be incorporated into synthetic vesicles to create programmable motility.

The Choi group designed a synthetic lipid cell decorated with DNA walkers and demonstrated dynamic surface migration.[98] In this study, the vesicles were modified with DNA strands via click chemistry and autonomously migrated on glass substrates functionalized with RNA fuel strands. They used an enzyme-powered burnt-bridge mechanism (Figure 3b), like Salaita's work. Initial DNA/RNA complexes immobilize the protocells on the surface. Then the RNase enzyme cleaves the RNA, which releases the DNA from the previous binding. Thus, the DNA strand finds new RNA fuels for hybridization. Repeating this process moves the vesicle autonomously and processively, traveling about 20 μm over 10 h. A random walk model with variable steps and velocities was used to describe the DNA-driven protocell movement. Further, mechanistic studies were performed to elucidate the design parameters that govern the motion performance, including walker design and environmental conditions, such as salt and enzyme concentrations.

2.3. Collective Migration. Cells in nature can move either individually, in an uncoordinated manner (single cell migration), or collectively, in cohesive cell groups (collective migration). Single cell migration can be used to navigate through tissues (as done by immune cells) or to localize themselves in secondary growths or tissues (as done by cancer cells).[99] The solution- and surface-based movements are examples of single cell motility. Collective migration is the driving force behind tissue remodelling during embryonic morphogenesis and wound repair.[100,101] Invasive tumor cells also display collective motion.[99] Researchers have taken inspiration from the mechanisms of collective migration in nature and tried to develop similar mechanisms in synthetic cells.

The mechanisms of collective migration are more complex and less developed as compared to those of single cell motion.[99] Nevertheless, efforts have been made to mimic collective motility behaviors in synthetic cells. Such studies include synthetic microswimmers from bimetallic rods and microspheres,[62] catalytic Janus colloids,[102,103] thermophoretic Janus colloids,[104] bubble jets,[105] rotators,[106] self-propelled droplets,[107] and biomimetic microswimmers.[108] Notably, much less work has been performed by using lipid vesicles. One such study was reported by Qiu et al. as illustrated in Figure 4a.[109] They constructed GUVs and SUVs functionalized with two sets of unique DNA oligonucleotides and demonstrated their programmable aggregation. A number of small vesicles aggregated onto a giant vesicle upon the addition of molecules for "bind" signals (i.e., DNA strands that bind with oligonucleotides on both small and giant vesicles). The small vesicles were dissociated from the giant vesicle when "release" signals were introduced. An interesting aspect of this approach is that the collective movement was facilitated by DNA origami pores embedded in the vesicle membrane, which allowed for selective signal transport into and out of the vesicle. Only when the transmembrane channels are opened can an inactive, external signal (a DNA hairpin strand in their

https://doi.org/10.1021/acssynbio.3c00271
ACS Synth. Biol. 2023, 12, 2789−2801

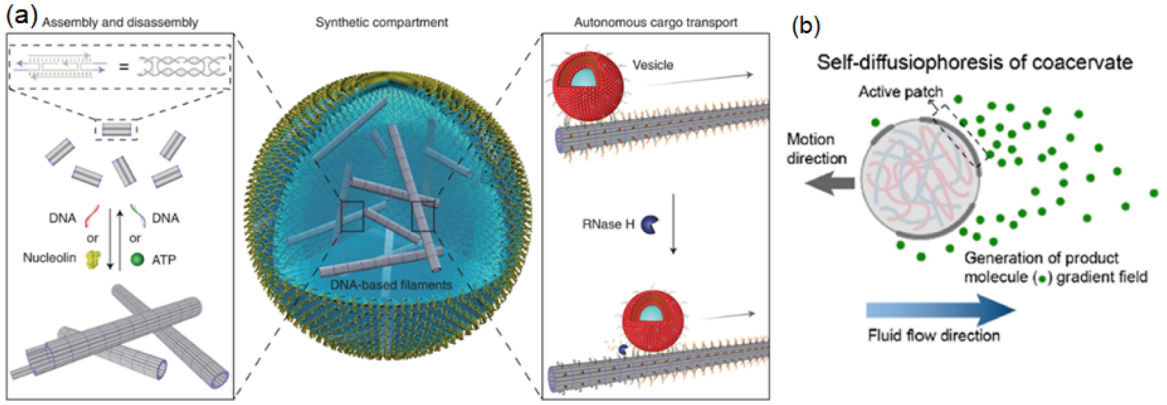

Figure 5. (a) Intracellular motility based on DNA-based filaments. Triggered by strand-displacement reactions or aptamer-target interactions, the filaments undergo programmed assembly and disassembly reactions. RNase H enzyme mediates directional motion of cargo (vesicles or nanoparticles) along the filament tracks. Reprinted with permission from ref 117. Published by 2022 Springer Nature Ltd. (b) Self-diffusiophoretic motion of coacervates. The active patches on the membrane of coacervates release product molecules which leads to an asymmetric product gradient field and hence, an osmotic imbalance. The fluid flow induced by the osmotic imbalance causes the movement of the coacervate. Reprinted with permission from ref 122. Published by American Chemical Society.

experiment) enter the GUV where it is transduced into an active signal by an enzyme (i.e., Exo III). The processed active signal can escape from the vesicle and induce the aggregation of SUVs onto the GUV. This study demonstrated feasibility to establish chemical pathways for communication among synthetic cells; thus, other complex collective motions and behaviors could be designed.

Another mechanism of collective migration uses the "leader-follower" states. Here, one cell leads the movement, and another follows it on the same path. The "leader" cell navigates the environment and uses mechanisms like chemical secretion and distortion of tracks to provide directional cues to the follower cell.[110] Some natural examples of the leader-follower pairs include neutrophils guiding T-cells, Drosophila border cells, and zebrafish lateral line primordium.[111] Pan et al. showed this directional motility of leader-follower pairs using synthetic lipid vesicles with DNA components.[112] Two sets of vesicles were designed, leader (red) and follower (green), each of which was functionalized with DNA walkers (Figure 4b). To implement coordinated behaviors, RNA fuels on the surfaces were designed with a hairpin loop. This hairpin fuel allows the DNA on the follower to move but hinders its movement due to the short length. Upon binding with the lead walker, the hairpin becomes opened, which allows for enzymatic vesicle movement. Then, the follower DNA is allowed to bind with its corresponding activated fuel. Since the follower experiences strong bias with activated fuels, the green vesicle will preferentially move along the activated fuels, that is, the trajectory of the leader. In this way, the follow vesicles "chase" the lead vesicle. This coordinated migration behavior is reminiscent of a neutrophil chasing a bacterium in our immune system.

2.4. Intracellular Motility. Intracellular motility is the fundamental method to transport various cargos, like essential molecules, organelles, and vesicles, necessary to maintain the normal functioning of the cell.[113] For example, neurons are heavily dependent on intracellular trafficking, and defects in this transport system can lead to neurogenerative and neurodevelopmental disorders.[114] Intracellular transport is responsible for maintaining the lipid bilayers, recycling of used proteins, providing membrane expansion in cell division, and storage of signal molecules.[115] Here, a combination of passive diffusion and molecular motor active transport moves the cargo ballistically along cytoskeletal filament networks.[116] Another important application of intracellular transport lies in cell apoptosis as it is necessary for the transport of apoptotic signaling pathway proteins.[113] Thus, motility of this type is important in synthetic cells.

Several studies have attempted to reconstitute intracellular motility inside lipid vesicles. Gopfrich, Liu, and their co-workers constructed synthetic cytoskeletons made of DNA filament networks as shown in Figure 5a.[117,118] Their design consisted of DNA tiles that self-assembled into filament networks which was inspired from the works of Green et al.[119] and Rothemund et al.[120] They aimed to control the filaments to emulate the functions and features of a natural cytoskeleton, which included guided vesicle transport inside a cell-sized confinement. To do this, they proposed a burnt-bridge mechanism that drives the directional movement along the DNA filaments. Sato et al. used DNA signals to develop an amoeba-like liposomal robot that can change its shape on demand.[121] The robot includes a body (a giant vesicle), a molecular motor system (kinesin and microtubules), and a control device to switch the shape from spherical to nonspherical and vice versa. A DNA signal binds to kinesin with functional moieties, thereby conjugating the motors on the lipid membrane. This prompts floating (inactive) microtubules to bind to immobilized kinesin, and their gliding on the membrane changes the shape of the GUV. It was also demonstrated that another DNA signal can reverse the process and restore the vesicle shape. This mechanism may be developed further to mimic the motion of an amoeba.

In another set of studies, Song et al. demonstrated the autonomous motion of coacervate micromotors confined inside a GUV.[122] They encapsulated enzyme-functionalized coacervates inside GUVs and studied the motile behavior of the compartmentalized motor system. The motility of the active coacervates was due to a stochastic process, where asymmetry is created when enzymes transiently cluster into patches on the particle surface, leading to enhanced diffusion. In this self-diffusiophoretic motion, the coacervate particles create a product gradient around the active patches by converting the fuel (H_2O_2 in this case), which causes an osmotic imbalance resulting in enhanced propulsion (Figure

https://doi.org/10.1021/acssynbio.3c00271
ACS Synth. Biol. 2023, 12, 2789−2801

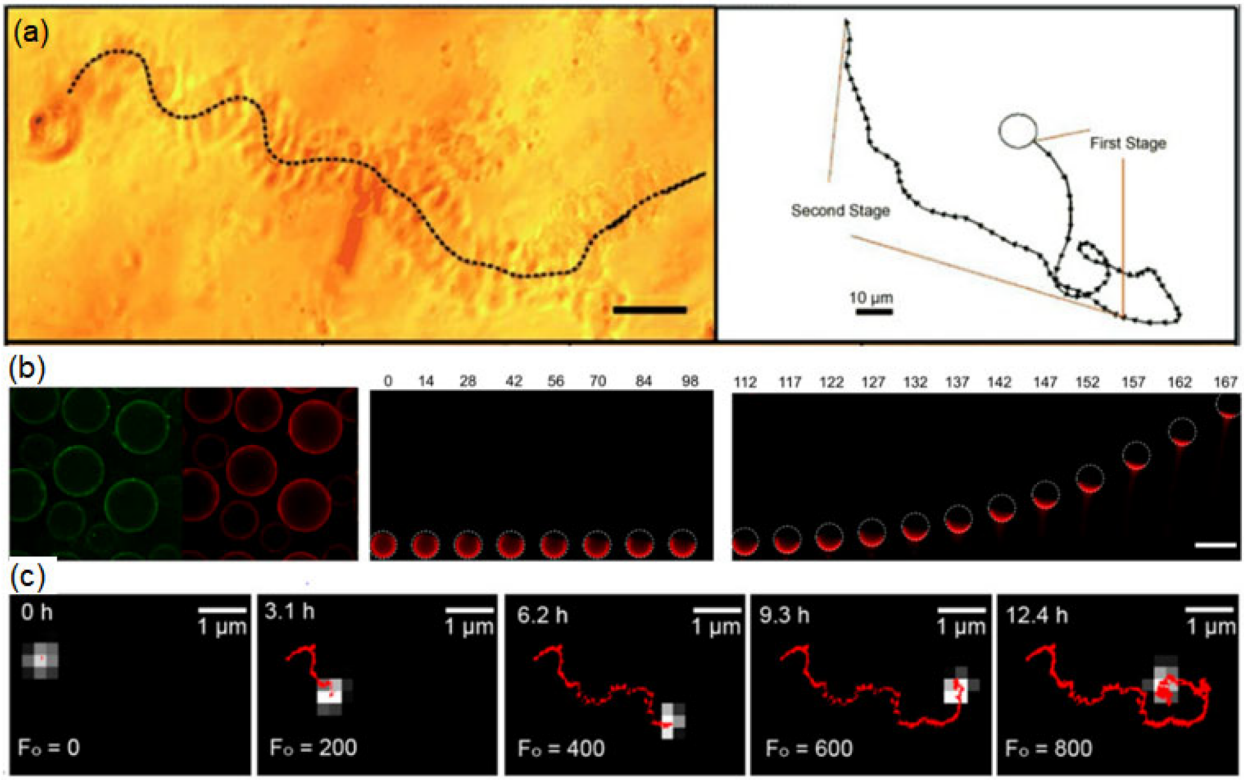

Figure 6. (a) Bright field imaging of a vesicle (left panel) and a representative trajectory on the right. Reprinted with permission from ref 59. Copyright 2011 John Wiley & Sons. (b) Epifluorescence images of movements of dextran-rich droplets with fluorescent vesicles at interfaces. The left panels show droplets labeled by fluorescent vesicles. The green channel uses calcein, while rhodamine dye was used for red. The right panel demonstrates the movement recorded with fluorescence imaging labeled with time in seconds. Scale bar: 20 μm. Reprinted with permission from ref 70. Published by 2021 Springer Nature Ltd. (c) Time-lapse imaging of a surface-migrating vesicle captured by TIRF microscopy. Protocell is shown in black and white colors. The trajectory of the particle is extracted by fitting to a Gaussian function and plotted in red color. *Fo* is the Fourier number ($Fo = Dt/r^2$ where D is the diffusion coefficient, t is time, and r is the radius of the vesicle) indicating dimensionless time. Reprinted with permission from ref 112. Copyright 2019 American Chemical Society.

5b). Under high fuel concentrations, the coacervate motors traveled several micrometers, and their mean square displacement (MSD) showed active, dynamic behaviors. The enhanced self-propulsion was driven by the catalase-mediated decomposition of H_2O_2. Thus, the movements and trajectories strongly depend on the H_2O_2 concentration. In the absences of fuel, the particles traveled significantly shorter paths, with a less mean square displacement (MSD).

They also compared the MSD profiles of coacervates in GUV confinement with those in bulk solution. They found that the compartmentalized coacervates showed lower MSD values with and without fuel and that, in the presence of fuel, the MSD curve changed from concave-upward for the coacervates in bulk solution to nearly linear for the compartmentalized particles. This showed that the motion was restricted inside GUVs. Interestingly, they observed that the coacervate motion in smaller GUVs was compromised with high fuel concentrations due to the enhanced viscous drag forces. Hence, for the compartmentalized particles, motion is in the subdiffusion regime in the absence of fuel and normal diffusion with fuel. In contrast, the movement of the particles in bulk solution is Brownian motion in the absence of fuel and ballistic movement with fuel. The relative concentrations of the particles also affect their motion with decreased movement in higher concentrations. Motion of particles in confinement is chiefly governed by the hydrodynamic effect and the phoretic effect.[123] In the hydrodynamic effect, the velocity in a fluid flow decreases to zero near the boundaries, which leads to viscous drag. In the phoretic effect, the motion of the molecules is affected by the confinement boundary, as due to less space for diffusion, the product gradient around the particles is more pronounced and enhances motion. These phenomena compete to influence motion. The hydrodynamic effect dominates in the case of coacervates in GUVs which is suggested by the decrease in motion. In the absence of fuel, there is no product gradient, and hence, the phoretic effect is ruled out. The addition of fuel can partially counteract the drag by the hydrodynamic effect; however, the motion is still restricted in comparison to that of the particles in bulk solution.

3. METHODS OF CHARACTERIZATIONS AND ANALYSIS FOR SYNTHETIC CELL MOTILITY

To understand the dynamics of synthetic cell motility, it is necessary to characterize the protocells and record their movement. The protocells' size may be characterized by dynamic light scattering.[124] Size and morphology can be measured simultaneously by methods such as optical microscopy, scanning electron microscopy, and transmission electron microscopy.[125] To track the movement, various imaging methods have been used to record synthetic cells in solutions and on surfaces. Among the microscopic methods used to capture movement, bright field microscopy is the simplest approach. It requires only one transillumination light

https://doi.org/10.1021/acssynbio.3c00271
ACS Synth. Biol. 2023, 12, 2789−2801

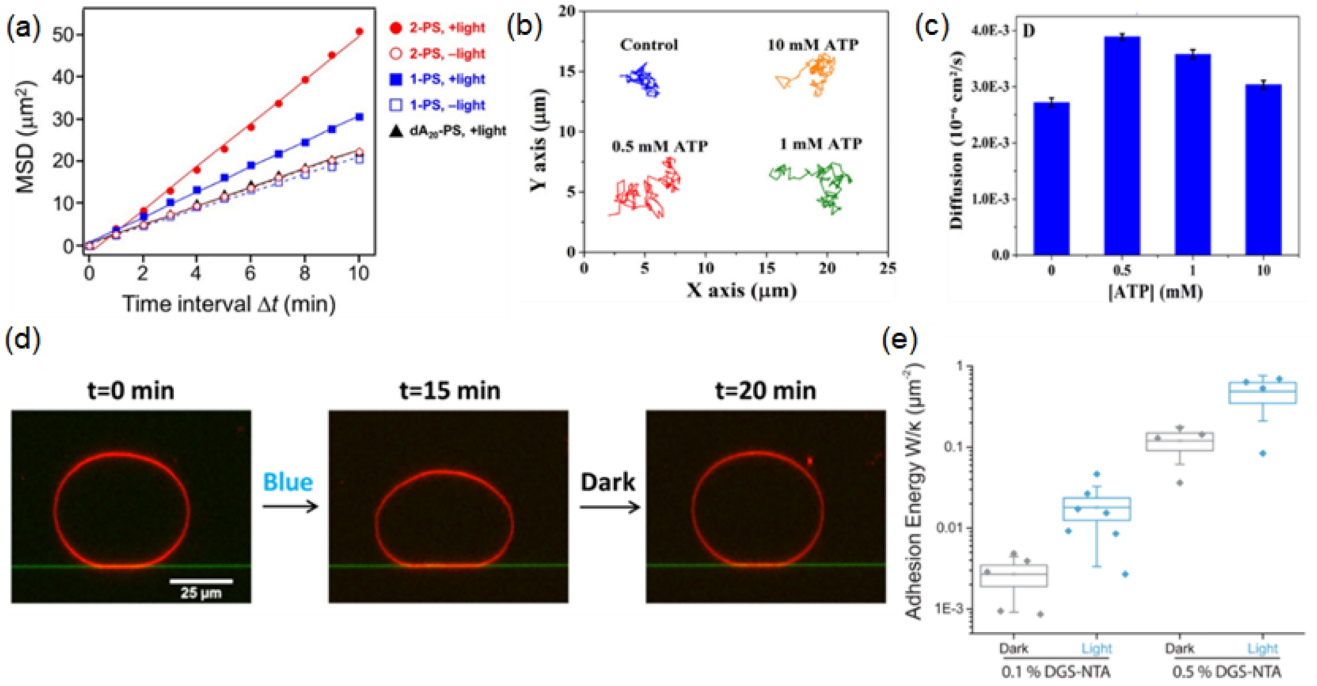

Figure 7. (a) MSD plot shows that vesicles with different compositions and conditions have different MSD scaling. As shown in Figure 3a, the vesicles have components on the membranes that can respond to light and create enhanced motility compared to random diffusion. Without light (hollow red circles and hollow blue squares) or without components (filled black triangles), the MSD plots slowly increase with relatively shallow slopes as a function of time. With light exposure (filled red circles and filled blue squares), the vesicles show increased motility with steeper slopes in the MSD plot. Reprinted with permission from ref (130). Published by 2021 Springer Nature Ltd. (b) Trajectories and (c) calculated diffusion coefficients of protocell motions with various ATP concentrations. As illustrated in Figure 2b, ATPase embedded in the membrane consumes ATP in the solution and generates propulsion, resulting in vesicle motility. Compared to the control (no ATP), the trajectories show more movements and diffusion coefficients are increased. Reprinted with permission from ref 72. Copyright 2019 American Chemical Society. (d) Fluorescence images of a giant lipid vesicle attached on a surface and (e) corresponding adhesion energy calculation. The morphological changes of the vesicle are guided by light with the mechanism explained in Figure 3a. The components on the liposome membrane respond to light irradiation and cause attachment or detachment from the surface, generating movements. The adhesion energy is calculated based on morphologies, where the surface tensions can be evaluated from the contact angles and integrated for the adhesion energy. The energy differences show that the conjugate DGS-NTA can respond to illumination and provide energy to the liposome so that they contact with the surface as the adhesion energies change and move along with the light. Reprinted with permission from ref 75. Copyright 2018 American Chemical Society.

source that goes through a condenser lens and focuses the light onto the samples, while an objective lens collects the light from the samples and magnifies images captured by a camera. Figure 6a shows the motions of lipid vesicles with intrinsic hydrogel networks recorded by optical tracking and illustrates that the vesicle traveled through the solution and left a trajectory.[59] The trajectories of locomotion were then collected for further analysis. Although bright field imaging is easy to use, there are obvious limitations such as low contrast of most liposome samples due to absorption of light and transparency of samples, which makes it difficult for them to be seen clearly. In addition, bright field imaging is limited by optical diffraction.

To push toward better images and higher resolution, fluorescence microscopy is commonly used. In fluorescence microscopy, the specimen is illuminated by light of a specific wavelength, and the fluorophores in the specimen absorb the incoming light as well as emit light of a different wavelength which will then be captured by a camera. The resulting images have higher contrasts and better quality compared with those of bright field images. The majority of the works used epifluorescence microscopy where the excitation light is transmitted through the samples and filtered by optical filters.[126] Embedment of fluorophores with protocells is an important aspect of successful imaging. The fluorophores can be encapsulated by the vesicles in the step of vesicle synthesis as depicted in the work of Ces group.[70] They incorporated calcein fluorophores in the synthesis and demonstrated clear images of droplets surrounded by calcein encapsulated vesicles, as shown in Figure 6b. They also showed that fluorophores can be modified on the vesicle membrane with fluorophore labeled lipids. In their experiment, they used a rhodamine modified phospholipid. The movement of the droplets were captured with the fluorescent vesicles. Similarly, Sen et al. used Chromeo P540 labeled ATPase in building liposomes.[72] It is clearly observed that fluorescence appeared on the outer edges of the synthetic cells. Their movements were recorded and extracted with trajectory analysis software and characterized further. One of the drawbacks of epifluorescence is that both fluorophores in and out of focus will be exposed to the excitation light and contribute to the images captured. This results in a relatively low signal-to-noise ratio.

To resolve this particular weakness, total internal reflection fluorescence (TIRF) microscopy has been introduced.[127] In the TIRF mode, the excitation light no longer passes through the sample; instead, it is shone at a specific angle which causes total reflection on the glass slide and generates an illumination field with depth between 30 and 300 nm. Dyes out of the field will not be excited and thus will not emit fluorescence. This leads to a significantly high signal-to-noise ratio. Jing et al. used TIRF measurement to capture the movements of protocells.[112]

https://doi.org/10.1021/acssynbio.3c00271
ACS Synth. Biol. 2023, 12, 2789−2801

Rhodamine modified lipids were used as a fluorescent probe embedded in the membrane of the vesicles. The trajectories were recorded and extracted with a point spread function (PSF). For intracellular imaging, the dimensions are usually in nanometers, which calls for methods with higher resolution. For example, Zhan et al. used stimulated emission depletion microscopy for measurement of vesicles moving on filaments inside a synthetic cell.[117] This method functions by depleting fluorescence in certain regions of the sample while leaving a center focal spot active to emit fluorescence, thus achieving super-resolution. Other super-resolution microscopy methods, such as photoactivated localization microscopy[128] and stochastic optical reconstruction microscopy,[129] may also be used according to the situation. These imaging methods provide powerful tools to collect large quantities of data on synthetic cell movements, which set the foundation for dynamic studies.

Acquired raw images need to be further analyzed to extract essential information on motion. Typically, captured protocell images are fitted with PSF (commonly used as a Gaussian function) via ImageJ or other software. Their localizations are determined by center positions, which then form time-lapse series that are used as trajectories of individual particles. The trajectories can provide many statistical insights into the motion. The most obvious characteristics include velocities and travel distances, which for synthetic cells fall on the micrometer scale and are comparable to natural cells. Other commonly used analyses include mean squared displacement (MSD) and diffusion coefficient. MSD is calculated by

$$\mathrm{MSD} = [\mathbf{r}(t + \Delta t) - \mathbf{r}(t)]^2 \sim t^{\alpha}$$

where Δt is time interval and $\mathbf{r}(t) = (x(t),y(t))$ is the vector position of the protocell at time t. MSD describes the deviation of particles away from the reference positions over time. This can be used as a measure of motion compared with standard Brownian motion (exponent coefficient $\alpha = 1$) and ballistic motion ($\alpha = 2$). It is useful to make a distinction between simple random motion and biased motion with enhanced motility. Matsuura et al.[130] used liposomes attached with peptides asymmetrically which generate Marangoni effect-powered motion, as shown in Figure 7a. They recorded videos of moving liposomes and analyzed their trajectories. The calculated MSD values of liposomes showed differences among particles with different fiber formations. The other important characteristic is the diffusion coefficient of the synthetic cells. Diffusion coefficient is a proportionality constant describing the molar flux due to particle diffusion and the gradient in the concentration of the species. In a large time scale, the diffusion coefficient is proportional to the slope of MSD-t plot in theory, while in actual experiments fluorescence correlation spectroscopy is often used to measure the diffusion coefficient.[131] This method records the intensity signal of illuminated samples over time, and the signal is computed to generate autocorrelation, which can then be fitted to calculate the diffusion coefficient and classify the diffusion into types such as normal diffusion, anomalous diffusion, etc. In the ATPase aided design, Sen et al. used this method to determine the diffusion coefficients of vesicles under different ATP concentrations and compared their dynamic features as demonstrated in Figure 7b.[72]

Further statistical features may be extracted from trajectories as Du et al. provided a continuous time random walk model.[98] In their dynamic model, the distributions of time and length of moving steps were calculated from segmented trajectories. The model showed that these statistical features can be used to predict different motion types of particles. This provides guidance to design particles with preferences toward different motion behaviors. For surface-based locomotion, the morphology of protocells contacting the substrate also imparts useful information. For example, Wegner et al. demonstrated that the morphology of a giant vesicle can be used to calculate the adhesion energy as shown in Figure 7c.[75,132] They showed the difference between attachment and detachment of the vesicles and the fact that adhesion energy changes with control over chemical concentrations. In summary, these in-depth analyses provide insights into dynamic features of synthetic motility and may offer vision for future designs of more powerful motors.

4. CONCLUDING REMARKS

In this review, we discuss one of the most important features of a cell, motility. Cellular motility involves the movement of cells or intracellular cargo from an initial site to a destination. It is vital for the occurrence of other cellular functions as well, and when this function is hampered, the results may be catastrophic in cell physiology. Numerous mechanisms have been proposed to describe the motility of natural cells, including electrical, mechanical, chemical, or conformational change driven motility. These cues need to be sensed, transmitted, and acted upon. These mechanisms have become a source of inspiration for motility in synthetic cells. Synthetic cell motility in two dimensions comprises membrane protrusions, adhesion to surface, and contractility and detachment. These codependent steps have been successfully reconstituted in synthetic cells. Despite the similarity of liposomes to biological cells, studies of reconstitution of motility using vesicles are still limited. Reconstitution mechanisms used in other types of synthetic cells can be explored with vesicles. For instance, Sasaki et al. developed artificial cilia from a reconstituted model of a biomolecular motor system of microtubule/kinesin using polystyrene beads.[133] The artificial cilia exhibited a beating motion upon consumption of chemical energy by kinesins and could be interesting to explore with liposomes.

Single cell motility can be classified into solution-based or surface-based. Various mechanisms developed for solution-based motility require specific environmental conditions or have limited synthesis methods that can restrain their applications. In surface-based motility, the protocells attach and detach from the surfaces, while the conformational changes help them gain directionality. Morphological changes controlled by temperature and light have been demonstrated as discussed above, and further investigation of these mechanisms could lead to novel applications in the study of protocells. Recently, DNA nanotechnology has been utilized for surface-based migration, as it offers high programmability, controllability, and flexibility in design. Thus, incorporating DNA self-assembly schemes into protocell motility is another lucrative area to explore. Cell motility can also be coordinated in the form of collective migration and has been achieved so far by using synthetic microswimmers, programmable cell aggregations, and leader-follower mechanisms. Developing autonomous microswimmers using liposomes could prove to be a promising research in this direction. In summary, we assert that further studies in the area of cell motility based on lipid vesicles are required and will have immense significance in fundamental research in synthetic biology as well as targeted drug delivery, intercellular artificial signaling, cargo transport,

https://doi.org/10.1021/acssynbio.3c00271
ACS Synth. Biol. 2023, 12, 2789−2801

and biomimicry. Developing reliable pathways for motility whose speeds and directionality rival those of biological cells would not only help us understand biological mechanisms but would also be a step toward developing synthetic life.

AUTHOR INFORMATION

Corresponding Author

Jong Hyun Choi − *School of Mechanical Engineering, Purdue University, West Lafayette, Indiana 47907, United States;* orcid.org/0000-0002-0507-3052; Email: jchoi@purdue.edu

Authors

Aishwary Shrivastava − *School of Mechanical Engineering, Purdue University, West Lafayette, Indiana 47907, United States*

Yancheng Du − *School of Mechanical Engineering, Purdue University, West Lafayette, Indiana 47907, United States*

Harshith K. Adepu − *School of Mechanical Engineering, Purdue University, West Lafayette, Indiana 47907, United States*

Ruixin Li − *School of Mechanical Engineering, Purdue University, West Lafayette, Indiana 47907, United States;* orcid.org/0000-0002-9079-1138

Anirudh S. Madhvacharyula − *School of Mechanical Engineering, Purdue University, West Lafayette, Indiana 47907, United States*

Alexander A. Swett − *School of Mechanical Engineering, Purdue University, West Lafayette, Indiana 47907, United States;* orcid.org/0009-0007-3391-3614

Complete contact information is available at: https://pubs.acs.org/10.1021/acssynbio.3c00271

Notes

The authors declare no competing financial interest.

ACKNOWLEDGMENTS

We acknowledge the support from the U.S. National Science Foundation (NSF) under award no. 2025187 and 2134603 (motility mechanisms) and the U.S. Department of Energy (DOE), Office of Science, Basic Energy Sciences (BES), under award no. DE-SC0020673 (methods of characterization and analysis).

REFERENCES

(1) Buddingh, B. C.; van Hest, J. C. M. Artificial Cells: Synthetic Compartments with Life-like Functionality and Adaptivity. *Acc. Chem. Res.* **2017**, *50*, 769−777.

(2) Wang, L.; Song, S.; van Hest, J.; Abdelmohsen, L. K.; Huang, X.; Sánchez, S. Biomimicry of Cellular Motility and Communication Based on Synthetic Soft-Architectures. *Small* **2020**, *16*, 1907680.

(3) Blain, J. C.; Szostak, J. W. Progress Toward synthetic cells. *Annual review of biochemistry* **2014**, *83*, 615−640.

(4) Guindani, C.; da Silva, L. C.; Cao, S.; Ivanov, T.; Landfester, K. Synthetic Cells: From Simple Bio-Inspired Modules to Sophisticated Integrated Systems. *Angew. Chem.* **2022**, *134*, No. e202110855.

(5) Gánti, T. *The principles of life*; Oxford University Press, 2003.

(6) Stano, P. Is research on "Synthetic Cells" moving to the next level? *Life* **2019**, *9*, 3.

(7) Wang, X.; Wu, S.; Tang, T.-Y. D.; Tian, L. Engineering strategies for sustainable synthetic cells. *Trends in Chemistry* **2022**, *4*, 1106.

(8) Rideau, E.; Dimova, R.; Schwille, P.; Wurm, F. R.; Landfester, K. Liposomes and polymersomes: a comparative review towards cell mimicking. *Chem. Soc. Rev.* **2018**, *47*, 8572−8610.

(9) Walde, P.; Cosentino, K.; Engel, H.; Stano, P. Giant vesicles: preparations and applications. *ChemBioChem.* **2010**, *11*, 848−865.

(10) Wang, X.; Tian, L.; Ren, Y.; Zhao, Z.; Du, H.; Zhang, Z.; Drinkwater, B. W.; Mann, S.; Han, X. Chemical Information Exchange in Organized Protocells and Natural Cell Assemblies with Controllable Spatial Positions. *Small* **2020**, *16*, No. e1906394.

(11) Li, M.; Harbron, R. L.; Weaver, J. V.; Binks, B. P.; Mann, S. Electrostatically gated membrane permeability in inorganic protocells. *Nat. Chem.* **2013**, *5*, 529−536.

(12) Huang, X.; Li, M.; Green, D. C.; Williams, D. S.; Patil, A. J.; Mann, S. Interfacial assembly of protein-polymer nano-conjugates into stimulus-responsive biomimetic protocells. *Nat. Commun.* **2013**, *4*, 1−9.

(13) Li, M.; Huang, X.; Tang, T. Y.; Mann, S. Synthetic cellularity based on non-lipid micro-compartments and protocell models. *Curr. Opin Chem. Biol.* **2014**, *22*, 1−11.

(14) Hosta-Rigau, L.; York-Duran, M. J.; Zhang, Y.; Goldie, K. N.; Stadler, B. Confined multiple enzymatic (cascade) reactions within poly (dopamine)-based capsosomes. *ACS Appl. Mater. Interfaces* **2014**, *6*, 12771−12779.

(15) Yadavalli, S. S.; Xiao, Q.; Sherman, S. E.; Hasley, W. D.; Klein, M. L.; Goulian, M.; Percec, V. Bioactive cell-like hybrids from dendrimersomes with a human cell membrane and its components. *Proc. Natl. Acad. Sci. U. S. A.* **2019**, *116*, 744−752.

(16) Kamat, N. P.; Katz, J. S.; Hammer, D. A. Engineering polymersome protocells. *journal of physical chemistry letters* **2011**, *2*, 1612−1623.

(17) Jiang, W.; Zhou, Y.; Yan, D. Hyperbranched polymer vesicles: from self-assembly, characterization, mechanisms, and properties to applications. *Chem. Soc. Rev.* **2015**, *44*, 3874−3889.

(18) Mason, A. F.; Thordarson, P. Polymersomes as protocellular constructs. *J. Polym. Sci., Part A: Polym. Chem.* **2017**, *55*, 3817−3825.

(19) van Stevendaal, M.; Vasiukas, L.; Yewdall, N. A.; Mason, A. F.; van Hest, J. C. M. Engineering of Biocompatible Coacervate-Based Synthetic Cells. *ACS Appl. Mater. Interfaces* **2021**, *13*, 7879−7889.

(20) Itel, F.; Najer, A.; Palivan, C. G.; Meier, W. Dynamics of Membrane Proteins within Synthetic Polymer Membranes with Large Hydrophobic Mismatch. *Nano Lett.* **2015**, *15*, 3871−3878.

(21) Jesorka, A.; Orwar, O. Liposomes: technologies and analytical applications. *Annu. Rev. Anal Chem. (Palo Alto Calif)* **2008**, *1*, 801−832.

(22) Rottet, S.; Iqbal, S.; Beales, P. A.; Lin, A.; Lee, J.; Rug, M.; Scott, C.; Callaghan, R. Characterisation of Hybrid Polymersome Vesicles Containing the Efflux Pumps NaAtm1 or P-Glycoprotein. *Polymers* **2020**, *12*, 1049.

(23) Le Meins, J.-F.; Schatz, C.; Lecommandoux, S.; Sandre, O. Hybrid polymer/lipid vesicles: state of the art and future perspectives. *Mater. Today* **2013**, *16*, 397−402.

(24) Bolinger, P. Y.; Stamou, D.; Vogel, H. An integrated self-assembled nanofluidic system for controlled biological chemistries. *Angew. Chem., Int. Ed. Engl.* **2008**, *47*, 5544−5549.

(25) Dwidar, M.; Seike, Y.; Kobori, S.; Whitaker, C.; Matsuura, T.; Yokobayashi, Y. Programmable Artificial Cells Using Histamine-Responsive Synthetic Riboswitch. *J. Am. Chem. Soc.* **2019**, *141*, 11103−11114.

(26) Kita, H.; Matsuura, T.; Sunami, T.; Hosoda, K.; Ichihashi, N.; Tsukada, K.; Urabe, I.; Yomo, T. Replication of genetic information with self-encoded replicase in liposomes. *Chembiochem* **2008**, *9*, 2403−2410.

(27) Noireaux, V.; Libchaber, A. A vesicle bioreactor as a step toward an artificial cell assembly. *Proc. Natl. Acad. Sci. U. S. A.* **2004**, *101*, 17669−17674.

(28) Lentini, R.; Martin, N. Y.; Forlin, M.; Belmonte, L.; Fontana, J.; Cornella, M.; Martini, L.; Tamburini, S.; Bentley, W. E.; Jousson, O.; Mansy, S. S. Two-Way Chemical Communication between Artificial and Natural Cells. *ACS Cent Sci.* **2017**, *3*, 117−123.

(29) Hardy, M. D.; Yang, J.; Selimkhanov, J.; Cole, C. M.; Tsimring, L. S.; Devaraj, N. K. Self-reproducing catalyst drives repeated

phospholipid synthesis and membrane growth. *Proc. Natl. Acad. Sci. U. S. A.* **2015**, *112*, 8187−8192.
(30) Castro, J. M.; Sugiyama, H.; Toyota, T. Budding and Division of Giant Vesicles Linked to Phospholipid Production. *Sci. Rep* **2019**, *9*, 165.
(31) Miele, Y.; Medveczky, Z.; Hollo, G.; Tegze, B.; Derenyi, I.; Horvolgyi, Z.; Altamura, E.; Lagzi, I.; Rossi, F. Self-division of giant vesicles driven by an internal enzymatic reaction. *Chem. Sci.* **2020**, *11*, 3228−3235.
(32) SenGupta, S.; Parent, C. A.; Bear, J. E. The principles of directed cell migration. *Nat. Rev. Mol. Cell Biol.* **2021**, *22*, 529−547.
(33) Pizzagalli, D. U.; Pulfer, A.; Thelen, M.; Krause, R.; Gonzalez, S. F. In Vivo Motility Patterns Displayed by Immune Cells Under Inflammatory Conditions. *Front Immunol* **2022**, *12*, 804159.
(34) Reig, G.; Pulgar, E.; Concha, M. L. Cell migration: from tissue culture to embryos. *Development* **2014**, *141*, 1999−2013.
(35) Li, L.; He, Y.; Zhao, M.; Jiang, J. Collective cell migration: Implications for wound healing and cancer invasion. *Burns Trauma* **2013**, *1*, 21−26.
(36) Kumar, B.; Patil, A. J.; Mann, S. Enzyme-powered motility in buoyant organoclay/DNA protocells. *Nat. Chem.* **2018**, *10*, 1154−1163.
(37) Bartelt, S. M.; Steinkuhler, J.; Dimova, R.; Wegner, S. V. Light-Guided Motility of a Minimal Synthetic Cell. *Nano Lett.* **2018**, *18*, 7268−7274.
(38) Jeong, S.; Nguyen, H. T.; Kim, C. H.; Ly, M. N.; Shin, K. Toward artificial cells: novel advances in energy conversion and cellular motility. *Adv. Funct. Mater.* **2020**, *30*, 1907182.
(39) Nakamura, S.; Minamino, T. Flagella-driven motility of bacteria. *Biomolecules* **2019**, *9*, 279.
(40) Schmidt, E. P.; Lee, W. L.; Zemans, R. L.; Yamashita, C.; Downey, G. P. On, around, and through: neutrophil-endothelial interactions in innate immunity. *Physiology* **2011**, *26*, 334−347.
(41) Hosking, E. R.; Vogt, C.; Bakker, E. P.; Manson, M. D. The Escherichia coli MotAB proton channel unplugged. *Journal of molecular biology* **2006**, *364*, 921−937.
(42) Mogilner, A.; Oster, G. Cell motility driven by actin polymerization. *Biophysical journal* **1996**, *71*, 3030−3045.
(43) Siton-Mendelson, O.; Bernheim-Groswasser, A. Toward the reconstitution of synthetic cell motility. *Cell adhesion & migration* **2016**, *10*, 461−474.
(44) Veksler, A.; Gov, N. S. Phase transitions of the coupled membrane-cytoskeleton modify cellular shape. *Biophysical journal* **2007**, *93*, 3798−3810.
(45) Mogilner, A.; Oster, G. Cell motility driven by actin polymerization. *Biophys. J.* **1996**, *71*, 3030−3045.
(46) Barnhart, E. L.; Lee, K.-C.; Keren, K.; Mogilner, A.; Theriot, J. A. An adhesion-dependent switch between mechanisms that determine motile cell shape. *PLoS biology* **2011**, *9*, No. e1001059.
(47) Nakamura, M.; Chen, L.; Howes, S. C.; Schindler, T. D.; Nogales, E.; Bryant, Z. Remote control of myosin and kinesin motors using light-activated gearshifting. *Nature Nanotechnol.* **2014**, *9*, 693−697.
(48) Borejdo, J.; Burlacu, S. Measuring orientation of actin filaments within a cell: orientation of actin in intestinal microvilli. *Biophysical journal* **1993**, *65*, 300−309.
(49) Chaffey, N.; Alberts, B.; Johnson, A.; Lewis, J.; Raff, M.; Roberts, K.; Walter, P. *Molecular biology of the cell*, 4th ed.; Oxford University Press, 2003.
(50) Svoboda, K.; Schmidt, C. F.; Schnapp, B. J.; Block, S. M. Direct Observation of Kinesin Stepping by Optical Trapping Interferometry. *Nature* **1993**, *365*, 721−727.
(51) Vale, R. D.; Funatsu, T.; Pierce, D. W.; Romberg, L.; Harada, Y.; Yanagida, T. Direct observation of single kinesin molecules moving along microtubules. *Nature* **1996**, *380*, 451−453.
(52) DeWitt, M. A.; Chang, A. Y.; Combs, P. A.; Yildiz, A. Cytoplasmic dynein moves through uncoordinated stepping of the AAA+ ring domains. *Science* **2012**, *335*, 221−225.
(53) Lin, J.; Okada, K.; Raytchev, M.; Smith, M. C.; Nicastro, D. Structural mechanism of the dynein power stroke. *Nature cell biology* **2014**, *16*, 479−485.
(54) Qiu, W.; Derr, N. D.; Goodman, B. S.; Villa, E.; Wu, D.; Shih, W.; Reck-Peterson, S. L. Dynein achieves processive motion using both stochastic and coordinated stepping. *Nature structural & molecular biology* **2012**, *19*, 193−200.
(55) Jarrell, K. F.; McBride, M. J. The surprisingly diverse ways that prokaryotes move. *Nature reviews microbiology* **2008**, *6*, 466−476.
(56) Insua, I.; Montenegro, J. Synthetic supramolecular systems in life-like materials and protocell models. *Chem.* **2020**, *6*, 1652−1682.
(57) Saper, G.; Hess, H. Synthetic systems powered by biological molecular motors. *Chem. Rev.* **2020**, *120*, 288−309.
(58) Sauter, D.; Schröter, M.; Frey, C.; Weber, C.; Mersdorf, U.; Janiesch, J. W.; Platzman, I.; Spatz, J. P. Artificial Cytoskeleton Assembly for Synthetic Cell Motility. *Macromol. Biosci.* **2023**, *23*, 2200437.
(59) Krishna Kumar, R.; Yu, X.; Patil, A. J.; Li, M.; Mann, S. Cytoskeletal-like Supramolecular Assembly and Nanoparticle-Based Motors in a Model Protocell. *Angew. Chem.* **2011**, *123*, 9515−9519.
(60) van Stevendaal, M. H.; van Hest, J. C.; Mason, A. F. Functional Interactions Between Bottom-Up Synthetic Cells and Living Matter for Biomedical Applications. *ChemSystemsChem.* **2021**, *3*, No. e2100009.
(61) Sengupta, S.; Ibele, M. E.; Sen, A. Fantastic voyage: designing self-powered nanorobots. *Angew. Chem., Int. Ed.* **2012**, *51*, 8434−8445.
(62) Paxton, W. F.; Sundararajan, S.; Mallouk, T. E.; Sen, A. Chemical locomotion. *Angew. Chem., Int. Ed.* **2006**, *45*, 5420−5429.
(63) Strulson, C. A.; Molden, R. C.; Keating, C. D.; Bevilacqua, P. C. RNA catalysis through compartmentalization. *Nature Chem.* **2012**, *4*, 941−946.
(64) Wang, L.; Lin, Y.; Zhou, Y.; Xie, H.; Song, J.; Li, M.; Huang, Y.; Huang, X.; Mann, S. Autonomic Behaviors in Lipase-Active Oil Droplets. *Angew. Chem.* **2019**, *131*, 1079−1083.
(65) Patino, T.; Feiner-Gracia, N.; Arque, X.; Miguel-Lopez, A.; Jannasch, A.; Stumpp, T.; Schaffer, E.; Albertazzi, L.; Sanchez, S. Influence of Enzyme Quantity and Distribution on the Self-Propulsion of Non-Janus Urease-Powered Micromotors. *J. Am. Chem. Soc.* **2018**, *140*, 7896−7903.
(66) Patino, T.; Porchetta, A.; Jannasch, A.; Llado, A.; Stumpp, T.; Schaffer, E.; Ricci, F.; Sanchez, S. Self-Sensing Enzyme-Powered Micromotors Equipped with pH-Responsive DNA Nanoswitches. *Nano Lett.* **2019**, *19*, 3440−3447.
(67) Wu, Y.; Wu, Z.; Lin, X.; He, Q.; Li, J. Autonomous movement of controllable assembled Janus capsule motors. *ACS Nano* **2012**, *6*, 10910−10916.
(68) Shao, J.; Abdelghani, M.; Shen, G.; Cao, S.; Williams, D. S.; van Hest, J. C. Erythrocyte membrane modified janus polymeric motors for thrombus therapy. *ACS Nano* **2018**, *12*, 4877−4885.
(69) Dindo, M.; Bevilacqua, A.; Soligo, G.; Monti, A.; Rosti, M.; Laurino, P. Chemotactic interactions drive migration of membraneless active droplets. *bioRxiv* **2023**, DOI: 10.1101/2023.04.25.538216.
(70) Zhang, S.; Contini, C.; Hindley, J. W.; Bolognesi, G.; Elani, Y.; Ces, O. Engineering motile aqueous phase-separated droplets via liposome stabilisation. *Nat. Commun.* **2021**, *12*, 1673.
(71) Testa, A.; Dindo, M.; Rebane, A. A.; Nasouri, B.; Style, R. W.; Golestanian, R.; Dufresne, E. R.; Laurino, P. Sustained enzymatic activity and flow in crowded protein droplets. *Nat. Commun.* **2021**, *12*, 6293.
(72) Ghosh, S.; Mohajerani, F.; Son, S.; Velegol, D.; Butler, P. J.; Sen, A. Motility of enzyme-powered vesicles. *Nano Lett.* **2019**, *19*, 6019−6026.
(73) Muddana, H. S.; Sengupta, S.; Mallouk, T. E.; Sen, A.; Butler, P. J. Substrate catalysis enhances single-enzyme diffusion. *J. Am. Chem. Soc.* **2010**, *132*, 2110−2111.
(74) Somasundar, A.; Ghosh, S.; Mohajerani, F.; Massenburg, L. N.; Yang, T.; Cremer, P. S.; Velegol, D.; Sen, A. Positive and negative

chemotaxis of enzyme-coated liposome motors. *Nat. Nanotechnol.* **2019**, *14*, 1129−1134.
(75) Bartelt, S. M.; Steinkühler, J.; Dimova, R.; Wegner, S. V. Light-guided motility of a minimal synthetic cell. *Nano Lett.* **2018**, *18*, 7268−7274.
(76) Ke, Y.; Castro, C.; Choi, J. H. Structural DNA Nanotechnology: Artificial Nanostructures for Biomedical Research. *Annu. Rev. Biomed. Eng.* **2018**, *20*, 375−401.
(77) Pan, J.; Li, F.; Cha, T.-G.; Chen, H.; Choi, J. H. Recent progress on DNA based walkers. *Curr. Opin. Biotechnol.* **2015**, *34*, 56−64.
(78) Rothemund, P. W. K. Folding DNA to Create Nanoscale Shapes and Patterns. *Nature* **2006**, *440*, 297−302.
(79) Douglas, S. M.; Dietz, H.; Liedl, T.; Hogberg, B.; Graf, F.; Shih, W. M. Self-assembly of DNA into Nanoscale Three-dimensional Shapes. *Nature* **2009**, *459*, 414−418.
(80) Ke, Y.; Ong, L. L.; Shih, W. M.; Yin, P. Three-dimensional Structures Self-assembled from DNA Bricks. *Science* **2012**, *338*, 1177−1183.
(81) Zhang, F.; Jiang, S.; Wu, S.; Li, Y.; Mao, C.; Liu, Y.; Yan, H. Complex wireframe DNA origami nanostructures with multi-arm junction vertices. *Nature Nanotechnol.* **2015**, *10*, 779.
(82) Du, Y.; Pan, J.; Choi, J. H. A Review on Optical Imaging of DNA Nanostructures and Dynamic Processes. *Methods and Applications in Fluorescence* **2019**, *7*, 012002.
(83) Li, F.; Cha, T. G.; Pan, J.; Ozcelikkale, Z.; Han, B.; Choi, J. H. DNA Walker-regulated Cancer Cell Growth Inhibition. *ChemBioChem.* **2016**, *17*, 1138−1141.
(84) Gu, H.; Chao, J.; Xiao, S. J.; Seeman, N. C. A Proximity-based Programmable DNA Nanoscale Assembly Line. *Nature* **2010**, *465*, 202−205.
(85) Simmel, F. C. Processive motion of bipedal DNA walkers. *ChemPhysChem* **2009**, *10*, 2593−2597.
(86) Shin, J.-S.; Pierce, N. A. A synthetic DNA walker for molecular transport. *J. Am. Chem. Soc.* **2004**, *126*, 10834−10835.
(87) Yin, P.; Yan, H.; Daniell, X. G.; Turberfield, A. J.; Reif, J. H. A Unidirectional DNAWalker That Moves Autonomously along a Track. *Angew. Chem., Int. Ed.* **2004**, *43*, 4906−4911.
(88) Yehl, K.; Mugler, A.; Vivek, S.; Liu, Y.; Zhang, Y.; Fan, M.; Weeks, E. R.; Salaita, K. High-speed DNA-based rolling motors powered by RNase H. *Nature Nanotechnol.* **2016**, *11*, 184.
(89) Bazrafshan, A.; Meyer, T.; Su, H.; Brockman, J. M.; Blanchard, A. T.; Piranej, S.; Duan, Y.; Ke, Y.; Salaita, K. Tunable DNA Origami Motors Translocate Ballistically Over μm Distances at nm/s Speeds. *Angew. Chem., Int. Ed.* **2020**, *59*, 9514.
(90) Pan, J.; Cha, T.-G.; Li, F.; Chen, H.; Bragg, N. A.; Choi, J. H. Visible/near-infrared subdiffraction imaging reveals the stochastic nature of DNA walkers. *Science advances* **2017**, *3*, No. e1601600.
(91) Wang, Z.-G.; Elbaz, J.; Willner, I. DNA machines: bipedal walker and stepper. *Nano Lett.* **2011**, *11*, 304−309.
(92) Qu, X.; Zhu, D.; Yao, G.; Su, S.; Chao, J.; Liu, H.; Zuo, X.; Wang, L.; Shi, J.; Wang, L.; Huang, W.; Pei, H.; Fan, C. An Exonuclease III-Powered, On-Particle Stochastic DNA Walker. *Angew. Chem., Int. Ed.* **2017**, *56*, 1855−1858.
(93) Lund, K.; Manzo, A.; Dabby, N.; Michelotti, N.; Johnson-Buck, A.; Nangreave, J.; Taylor, S.; Pei, R.; Stojanovic, M. N.; Walter, N. G.; Winfree, E.; Yan, H. Molecular Robots Guided by Prescriptive Landscapes. *Nature* **2010**, *465*, 206−210.
(94) Bath, J.; Green, S. J.; Turberfield, A. J. A Free-Running DNA Motor Powered by a Nicking Enzyme. *Angew. Chem.* **2005**, *44*, 4358−4361.
(95) Wickham, S. F. J.; Endo, M.; Katsuda, Y.; Hidaka, K.; Bath, J.; Sugiyama, H.; Turberfield, A. J. Direct Observation of Stepwise Movement of a Synthetic Molecular Transporter. *Nat. Nanotechnol.* **2011**, *6*, 166−169.
(96) Cha, T.-G.; Pan, J.; Chen, H.; Salgado, J.; Li, X.; Mao, C.; Choi, J. H. A synthetic DNA motor that transports nanoparticles along carbon nanotubes. *Nature Nanotechnol.* **2014**, *9*, 39−43.
(97) Cha, T. G.; Pan, J.; Chen, H.; Robinson, H. N.; Li, X.; Mao, C.; Choi, J. H. Design Principles of DNA Enzyme-Based Walkers: Translocation Kinetics and Photoregulation. *J. Am. Chem. Soc.* **2015**, *137*, 9429−9437.
(98) Du, Y.; Pan, J.; Qiu, H.; Mao, C.; Choi, J. H. Mechanistic Understanding of Surface Migration Dynamics with DNA Walkers. *J. Phys. Chem. B* **2021**, *125*, 507−517.
(99) Friedl, P.; Gilmour, D. Collective cell migration in morphogenesis, regeneration and cancer. *Nat. Rev. Mol. Cell Biol.* **2009**, *10*, 445−457.
(100) Lecaudey, V.; Gilmour, D. Organizing moving groups during morphogenesis. *Curr. Opin Cell Biol.* **2006**, *18*, 102−107.
(101) Poujade, M.; Grasland-Mongrain, E.; Hertzog, A.; Jouanneau, J.; Chavrier, P.; Ladoux, B.; Buguin, A.; Silberzan, P. Collective migration of an epithelial monolayer in response to a model wound. *Proc. Natl. Acad. Sci. U. S. A.* **2007**, *104*, 15988−15993.
(102) Liebchen, B.; Lowen, H. Synthetic Chemotaxis and Collective Behavior in Active Matter. *Acc. Chem. Res.* **2018**, *51*, 2982−2990.
(103) Uspal, W.; Popescu, M. N.; Dietrich, S.; Tasinkevych, M. Self-propulsion of a catalytically active particle near a planar wall: from reflection to sliding and hovering. *Soft Matter* **2015**, *11*, 434−438.
(104) de Buyl, P.; Kapral, R. Phoretic self-propulsion: a mesoscopic description of reaction dynamics that powers motion. *Nanoscale* **2013**, *5*, 1337−1344.
(105) Sanchez, S.; Solovev, A. A.; Harazim, S. M.; Deneke, C.; Feng Mei, Y.; Schmidt, O. G. The smallest man-made jet engine. *Chem. Rec.* **2011**, *11*, 367−370.
(106) Gotze, I. O.; Gompper, G. Dynamic self-assembly and directed flow of rotating colloids in microchannels. *Phys. Rev. E Stat Nonlin Soft Matter Phys.* **2011**, *84*, 031404.
(107) Thutupalli, S.; Seemann, R.; Herminghaus, S. Swarming behavior of simple model squirmers. *New J. Phys.* **2011**, *13*, 073021.
(108) Williams, B. J.; Anand, S. V.; Rajagopalan, J.; Saif, M. T. A. A self-propelled biohybrid swimmer at low Reynolds number. *Nat. Commun.* **2014**, *5*, 1−8.
(109) Qiu, H.; Li, F.; Du, Y.; Li, R.; Hyun, J. Y.; Lee, S. Y.; Choi, J. H. Programmable Aggregation of Artificial Cells with DNA Signals. *ACS Synth. Biol.* **2021**, *10*, 1268−1276.
(110) Rørth, P. Fellow travellers: emergent properties of collective cell migration. *EMBO reports* **2012**, *13*, 984−991.
(111) Schumacher, L. J.; Kulesa, P. M.; McLennan, R.; Baker, R. E.; Maini, P. K. Multidisciplinary approaches to understanding collective cell migration in developmental biology. *Open Biol.* **2016**, *6*, 160056.
(112) Pan, J.; Du, Y.; Qiu, H.; Upton, L. R.; Li, F.; Choi, J. H. Mimicking Chemotactic Cell Migration with DNA Programmable Synthetic Vesicles. *Nano Lett.* **2019**, *19*, 9138−9144.
(113) Li, B.; Dou, S.-X.; Yuan, J.-W.; Liu, Y.-R.; Li, W.; Ye, F.; Wang, P.-Y.; Li, H. Intracellular transport is accelerated in early apoptotic cells. *Proc. Natl. Acad. Sci. U. S. A.* **2018**, *115*, 12118−12123.
(114) Basu, H.; Ding, L.; Pekkurnaz, G.; Cronin, M.; Schwarz, T. L. Kymolyzer, a Semi-Autonomous Kymography Tool to Analyze Intracellular Motility. *Curr. Protoc Cell Biol.* **2020**, *87*, No. e107.
(115) Brown, E.; Van Weering, J.; Sharp, T.; Mantell, J.; Verkade, P. Capturing endocytic segregation events with HPF-CLEM. *Methods Cell Biol.* **2012**, *111*, 175−201.
(116) Ando, D.; Korabel, N.; Huang, K. C.; Gopinathan, A. Cytoskeletal Network Morphology Regulates Intracellular Transport Dynamics. *Biophys. J.* **2015**, *109*, 1574−1582.
(117) Zhan, P.; Jahnke, K.; Liu, N.; Gopfrich, K. Functional DNA-based cytoskeletons for synthetic cells. *Nat. Chem.* **2022**, *14*, 958−963.
(118) Jahnke, K.; Huth, V.; Mersdorf, U.; Liu, N.; Gopfrich, K. Bottom-up Assembly of Synthetic Cells with a DNA Cytoskeleton. *ACS Nano* **2022**, *16*, 7233−7241.
(119) Green, L. N.; Subramanian, H. K. K.; Mardanlou, V.; Kim, J.; Hariadi, R. F.; Franco, E. Autonomous dynamic control of DNA nanostructure self-assembly. *Nat. Chem.* **2019**, *11*, 510−520.
(120) Rothemund, P. W.; Ekani-Nkodo, A.; Papadakis, N.; Kumar, A.; Fygenson, D. K.; Winfree, E. Design and characterization of

https://doi.org/10.1021/acssynbio.3c00271
ACS Synth. Biol. 2023, 12, 2789−2801

programmable DNA nanotubes. *J. Am. Chem. Soc.* **2004**, *126*, 16344−16352.
(121) Sato, Y.; Hiratsuka, Y.; Kawamata, I.; Murata, S.; Nomura, S. M. Micrometer-sized molecular robot changes its shape in response to signal molecules. *Sci. Robot* **2017**, *2*, No. eaal3735.
(122) Song, S.; Llopis-Lorente, A.; Mason, A. F.; Abdelmohsen, L.; van Hest, J. C. M. Confined Motion: Motility of Active Microparticles in Cell-Sized Lipid Vesicles. *J. Am. Chem. Soc.* **2022**, *144*, 13831−13838.
(123) Yang, F.; Qian, S.; Zhao, Y.; Qiao, R. Self-diffusiophoresis of Janus catalytic micromotors in confined geometries. *Langmuir* **2016**, *32*, 5580−5592.
(124) Pecora, R. Dynamic light scattering measurement of nanometer particles in liquids. *J. Nanopart. Res.* **2000**, *2*, 123−131.
(125) Hayat, M. A.: *Principles and techniques of electron microscopy. Biological applications*; Edward Arnold., 1981.
(126) Paige, M.; Bjerneld, E.; Moerner, W. A Comparison of Through-the-Objective Total Internal Reflection Microscopy and Epifluorescence Microscopy for Single-Molecule Fluorescence Imaging. *Single Molecules* **2001**, *2*, 191−201.
(127) Axelrod, D. Total internal reflection fluorescence microscopy in cell biology. *Traffic* **2001**, *2*, 764−774.
(128) Shroff, H.; Galbraith, C. G.; Galbraith, J. A.; Betzig, E. Live-cell photoactivated localization microscopy of nanoscale adhesion dynamics. *Nat. Methods* **2008**, *5*, 417−423.
(129) Rust, M. J.; Bates, M.; Zhuang, X. Sub-diffraction-limit imaging by stochastic optical reconstruction microscopy (STORM). *Nat. Methods* **2006**, *3*, 793−796.
(130) Inaba, H.; Uemura, A.; Morishita, K.; Kohiki, T.; Shigenaga, A.; Otaka, A.; Matsuura, K. Light-induced propulsion of a giant liposome driven by peptide nanofibre growth. *Sci. Rep* **2018**, *8*, 6243.
(131) Petrasek, Z.; Schwille, P. Precise measurement of diffusion coefficients using scanning fluorescence correlation spectroscopy. *Biophys. J.* **2008**, *94*, 1437−1448.
(132) Seifert, U.; Lipowsky, R. Adhesion of vesicles. *Phys. Rev. A* **1990**, *42*, 4768−4771.
(133) Sasaki, R.; Kabir, A. M. R.; Inoue, D.; Anan, S.; Kimura, A. P.; Konagaya, A.; Sada, K.; Kakugo, A. Construction of artificial cilia from microtubules and kinesins through a well-designed bottom-up approach. *Nanoscale* **2018**, *10*, 6323−6332.

https://doi.org/10.1021/acssynbio.3c00271
ACS Synth. Biol. 2023, 12, 2789−2801